Dynamic Response of Inelastic Thick Plates

S. S. Rao*
Indian Institute of Technology, Kanpur, India
and
K. S. Raghavan†
Bharat Heavy Electricals Ltd., Hyderabad, India

The dynamic behavior of inelastic thick plates is investigated. A 36-degree-of-freedom rectangular finite element, which includes shear deformation effects and adequately represents associated boundary conditions, is developed. The accuracy of the element is established through comparison with available results for static deflection and natural frequencies. The yield surface is considered as a function of in-plane and transverse shear stresses. It is found that the contribution of the transverse shear stresses upon the plastic deformations is relatively small. The response of simply supported and clamped thick plates to impulse excitation is found and the results are compared with those obtained from thin plate theory.

Introduction

ALTHOUGH a considerable amount of research has been carried out in the area of dynamic inelastic behavior of structures in the past two decades, no work has been reported concerning the response of thick plates. The theory of thick plates or, more aptly, moderately thick plates, includes the effects of shear deformation and rotary inertia and has applications where 1) the thickness is large, 2) analysis of stress concentration around holes of the order of thickness is required, and 3) higher modes dominate the response. So far, most of the studies concerning the vibration of thick plates are limited in scope to the evaluation of natural frequencies.[1-4] Rock and Hinton[5] studied the transient elastic response by using a finite element based on the refined plate theory. No study, however, has been reported on dynamic inelastic behavior of thick plates.

In this paper, inelastic response of thick plates is studied by using finite-element idealization in space, followed by numerical integration of the equations of motion according to an initial strain approach. A new rectangular finite element based on Mindlin's plate theory is developed for this purpose.

Finite Elements for Thick Plates

Several possible approaches to derive finite-element expressions for thick plates have been explored in the past. Felippa[6] proposed a method in which the displacement field consists of only the transverse deflection as in thin plates. In this approach, the expressions for the moments are modified to account for the transverse shear and, because of this, the resulting element will not be a pure displacement model. However, no element was derived by him along the proposed lines. Pryor and Barker[3] developed a 20-degree-of-freedom finite-element stiffness matrix by defining a displacement field that consists of the transverse deflection and two shear rotations. An isoparametric thick plate element was given by Rock and Hinton.[5] This element has three independent displacement fields defining the transverse deflection and the two rotations, about the in-plane axes, of the normal to the middle plane. Each displacement has a corresponding degree of freedom at each of the eight nodes so that the element has 24 degrees-of-freedom in all.

Received Oct. 3, 1977; revision received Aug. 29, 1978.

Index category: Structural Dynamics.

*Professor, Dept. of Mechanical Engineering.
†Senior Design Engineer.

The element to be presented here is based on defining three independent displacement fields, as in the case of Rock and Hinton's element. However, here each displacement is defined in terms of three degrees-of-freedom at each node. In this manner, the resulting element allows a better representation of the boundary conditions. The basis of the present element is the Mindlin plate theory[1] in which lines normal to the middle plane remain straight, but not necessarily normal, after deformation. The displacement field $\{w\}$ is defined as:

$$\{w\} = \lfloor w_z \bar{\phi}_y \bar{\phi}_x \rfloor^T \tag{1}$$

where w_z is the transverse deflection of the middle plane and $\bar{\phi}_y$ and $\bar{\phi}_x$ are the rotations of the normal to the middle plane about the y and x axes, respectively. Each of these is a function of the in-plane coordiantes x and y as:

$$\{w\} = \begin{bmatrix} \lfloor N \rfloor & 0 & 0 \\ 0 & \lfloor N \rfloor & 0 \\ 0 & 0 & \lfloor N \rfloor \end{bmatrix} \begin{Bmatrix} \bar{u}_1 \\ \bar{u}_2 \\ \bar{u}_3 \end{Bmatrix} \tag{2}$$

where $\bar{u}_1, \bar{u}_2$, and $\bar{u}_3$ are the nodal displacement vectors that define the three displacements w_z, $\bar{\phi}_y$, and $\bar{\phi}_x$, respectively, and $\lfloor N \rfloor$ represents the phosen displacement functions. The generalized strains are the curvatures c_x, c_y, and c_{xy} and the effective shear rotations $\bar{\theta}_x$ and $\bar{\theta}_y$. These are given by

$$c_x = (\partial \bar{\phi}_y / \partial x) \tag{3a}$$

$$c_y = (\partial \bar{\phi}_x / \partial y) \tag{3b}$$

$$c_{xy} = (\partial \bar{\phi}_y / \partial y + \partial \bar{\phi}_x / \partial x) \tag{3c}$$

$$\bar{\theta}_x = (\partial w_z / \partial y - \bar{\phi}_x) \tag{3d}$$

$$\bar{\theta}_y = (\partial w_z / \partial x - \bar{\phi}_y) \tag{3e}$$

The strain-displacement relation is:

$$\{\epsilon\} = [B]\{u\} \tag{4}$$

where $\{\epsilon\}$ is the vector of generalized strains and $\{u\}$ is the nodal displacement vector consisting of $\{\bar{u}_1\}$, $\{\bar{u}_2\}$, and $\{\bar{u}_3\}$. The strain-displacement matrix $[B]$ is defined, using

Eqs. (3), as:

$$[B]=\begin{bmatrix} 0 & \lfloor N_x \rfloor & 0 \\ 0 & 0 & \lfloor N_y \rfloor \\ 0 & \lfloor N_y \rfloor & \lfloor N_x \rfloor \\ \lfloor N_x \rfloor & -\lfloor N \rfloor & 0 \\ \lfloor N_y \rfloor & 0 & -\lfloor N \rfloor \end{bmatrix} \tag{5}$$

where the subscripts x and y represent differentiation with respect to x and y, respectively.

The stress resultants that correspond to the generalized strains are the the moments M_x, M_y, and M_{xy} and shear resultants S_x and S_y. The generalized stresses $\{\sigma\}$ are defined as:

$$\{\sigma\}=\lfloor M_x \;\; M_y \;\; M_{xy} \;\; S_x \;\; S_y \rfloor^T \tag{6}$$

and the stress-strain relation is given by:

$$\{\sigma\}=[D]\{\epsilon\} \tag{7}$$

where $[D]$ is the elasticity matrix:

$$[D]=\begin{bmatrix} D_1 & D_2 & 0 & 0 & 0 \\ D_2 & D_1 & 0 & 0 & 0 \\ 0 & 0 & D_3 & 0 & 0 \\ 0 & 0 & 0 & S_1 & 0 \\ 0 & 0 & 0 & 0 & S_1 \end{bmatrix} \tag{8}$$

with

$$D_1=\frac{Eh^3}{12(1-\nu^2)}, \quad D_2=\nu D_1, \quad D_3=\frac{D_1(1-\nu)}{2}$$

and

$$S_1=\frac{Eh}{2(1+\nu)\alpha}$$

In these expressions, E and ν are Young's modulus and Poisson's ratio, h is the plate thickness, and α is the shear coefficient for which a value of $\alpha=6/5$, as suggested by Reissner,[7] is assigned.

By using Eqs. (5) and (6) and the usual procedure of finite-element theory,[8,9] the stiffness matrix $[k]$ can be derived as:

$$[k]=\int_{\text{area}} \begin{array}{c} \\ 1 \\ 2 \\ 3 \end{array} \begin{array}{c} \begin{array}{ccc} 1 & 2 & 3 \end{array} \\ \left[\begin{array}{ccc} N_x^T S_1 N_x & -N_x^T S_1 N & -N_y^T S_1 N \\ \hline & N_x^T D_1 N_x & N_x^T D_2 N_y \\ -N^T S_1 N_x & +N_y^T D_3 N_y & +N_y^T D_3 N_x \\ & +N^T S_1 N & \\ \hline & & N_y^T D_2 N_y \\ -N^T S_1 N_y & N_y^T D_2 N_x & +N_x^T D_3 N_x \\ & +N_x^T D_3 N_y & +N^T S_1 N \end{array}\right] \end{array} dA$$

In Eq. (9), the symbol $\lfloor \; \rfloor$ for row vector is omitted for simplicity, and the partitions 1, 2, and 3 refer to the degree of freedom $\{\bar{u}_1\}$, $\{\bar{u}_2\}$, and $\{\bar{u}_3\}$, respectively.

The inertial terms corresponding to the three displacements are uncoupled. From the general expression for mass matrix,[8] the mass matrices corresponding to $\{\bar{u}_1\}$, $\{\bar{u}_2\}$, and $\{\bar{u}_3\}$ can be derived independently. In the elements referring to $\{\bar{u}_2\}$ and $\{\bar{u}_3\}$, we substitute the rotary inertia term $\rho h^2/12$, where ρ is the mass density of the material. The element mass matrix $[m]$ is then given by:

$$[m]=\rho h \int_{\text{area}} \left[\begin{array}{c|c|c} N^T N & 0 & 0 \\ \hline 0 & \frac{h^2}{12} N^T N & 0 \\ \hline 0 & 0 & \frac{h^2}{12} N^T N \end{array}\right] dA \tag{10}$$

Equations (9) and (10) are the generalized expressions for the stiffness and mass matrices. From these, various finite elements can be derived depending on the shape of the element and the choice of the displacement functions $\lfloor N \rfloor$.

In the present paper, rectangular elements are used and Hermitian interpolation functions[10] for $\lfloor N \rfloor$ are substituted. The element has three degrees of freedom for each of the three displacements at each node—36 degrees of freedom in all. The degrees of freedom at each node are w_z, $\partial w_z/\partial x$, $\partial w_z/\partial y$, $\bar{\phi}_y$, $\partial\bar{\phi}_y/\partial x$, $\partial\bar{\phi}_y/\partial y$, $\bar{\phi}_x$, $\partial\bar{\phi}_x/\partial x$, $\partial\bar{\phi}_x/\partial y$.

The applicability of the present element was tested by computing static deflections and natural frequencies of simply supported plates for which results are available. A few of these results are presented in Table 1. The stiffness and mass matrices were generated on the computer by using numerical quadrature. The static deflection given by the present element is seen to be within 1% of the analytical result reported by Salerno and Goldberg.[11] Natural frequencies were computed by taking four elements in each quarter of the plate. The results are compared with those obtained by Rock and Hinton,[5] the Mindlin theory,[2] and the three-dimensional theory by Srinivas et al.[4] The results of the present element are seen to agree well with the analytical results. Moreover, the element is seen to be more accurate than the isoparametric element of Rock and Hinton, particularly for higher modes.

For clamped plates, the present element will give more accurate results than the element of Rock and Hinton, as the former can satisfy zero deflection, bending slope, and twist conditions

$$w_z=\frac{\partial w_z}{\partial x}=\bar{\phi}_y=\frac{\partial\bar{\phi}_y}{\partial y}=\bar{\phi}_x=\frac{\partial\bar{\phi}_x}{\partial x}=0 \quad \begin{array}{l}(\text{if the edge is}\\ \text{defined by } y=\text{constant})\end{array}$$

The present element retains the distinction between the total slope and the bending slope in defining the boundary conditions, unlike in the case of Rock and Hinton's element in which the nodal degrees of freedom are the transverse deflection and the two bending slopes.

Elastoplastic Response

The finite element developed in the previous section is used to obtain the inelastic response of thick plates. The equations of motion are written as:

$$[M]\{\ddot{U}\}+[K]\{U\}=\{F\}+\Sigma\{\Delta F_p\} \tag{11}$$

where $[M]$ and $[K]$ are the assembled mass and stiffness matrices and $\{U\}$ and $\{F\}$ are the vectors of nodal displacements and forces, respectively. The vector $\{\Delta F_p\}$ represents the equivalent incremental nodal loads that account for the plastic flow. The summation in Eq. (11) spans all the time intervals up to the current one while evaluatin the step-by-step response. It can be shown that at any given time step,[12]

$$\{\Delta F_p\}=\sum_j \{\Delta F_p\}_j \tag{12}$$

Table 1 Static deflections and natural frequencies of simply supported thick square plates

Static deflections under uniform pressure p
Values of $(\delta Eh^3/pa^4)$ for $\nu = 0.3$

a/h	Present element	Analytical result [11]	Thin plate
10	0.0467	0.0463	0.0444
5	0.0546	—	0.0444

Natural frequencies
Values of $\omega_{mn}(\rho h^2/G)^{1/2}$ for $\nu = 0.3$

a/h	m	n	Present element	Finite element [5]	Mindlin theory [2]	Three-dimensional theory [4]
10	1	1	0.0934	0.0931	0.0930	0.0937
10	1	2	0.2200	0.2237	0.2218	0.2226
10	2	2	0.3499	0.3384	0.3402	0.3420
10	1	3	0.4078	0.4312	0.4144	0.4177
10	2	3	0.5372	0.5379	0.5197	0.5239
10	3	3	0.7325	0.7611	0.6821	0.6889
5	1	1	0.3405	0.3407	0.3402	0.3421
5	2	1	0.7412	0.7493	0.7431	0.7511
5	2	2	1.0780	1.0564	1.0735	1.0890

where

$$\{\Delta F_p\}_j = \int_{V_j} [B]_j^T [D]\{\Delta\epsilon_p\}_j \cdot \mathrm{d\ vol} \tag{13}$$

Thus, the equivalent nodal load vector is obtained by assembling the vectors over all the elements. In Eq. (13), V_j is the volume of the jth element, $[B]_j$ the strain-displacement matrix, $\{\Delta\epsilon_p\}_j$ the vector of plastic components of incremental strains (a function of the spatial coordinates within the element), and $[D]$ the elasticity matrix. The evaluation of incremental loads thus involves computation of the plastic components of strain increments within each element as a function of its spatial coordinates. Before proceeding to the plastic analysis, the stress distribution across the thickness and yield criterion are presented.

The stress field defined in Eq. (6) consists of generalized values and is a function of the in-plane coordinates only. According to Drucker,[13] a unique yield criterion in terms of moment and the transverse shear resultant does not exist. The difficulty can be overcome by discarding the generalized variables and by defining the elastic-plastic stress-strain relation in terms of the unit stresses and strains, thereby retaining the variation of stresses across the thickness also. Across the depth, at any point, the stress field consists of three in-plane stresses—σ_x, σ_y, and σ_{xy}—and two transverse shear stresses—σ_{xz} and σ_{yz}. The corresponding strains are ϵ_x, ϵ_y, ϵ_{xy}, ϵ_{xz}, and ϵ_{yz}. The elasticity matrix is given by:

$$[D] = \frac{E}{1-\nu^2}\begin{bmatrix} 1 & & & & & \\ \nu & 1 & & & & \text{Symmetric} \\ 0 & 0 & \frac{(1-\nu)}{2} & & & \\ 0 & 0 & 0 & \frac{(1-\nu)}{2} & & \\ 0 & 0 & 0 & 0 & \frac{(1-\nu)}{2} & \end{bmatrix} \tag{14}$$

The relation between the in-plane strains ϵ_x, ϵ_y, and ϵ_{xy} and the curvatures c_x, c_y, and c_{xy} is the same as in classical plate theory, that is

$$\epsilon_x = -zc_x \qquad \epsilon_y = -zc_y \qquad \epsilon_{xy} = -zc_{xy} \tag{15}$$

where z is the distance measured from the middle plane. The variation of transverse shear stresses σ_{xz} and σ_{yz} with z is parabolic[14] as:

$$\sigma_{xz} = \frac{3}{2}\frac{S_x}{h}\left(1 - \frac{4z^2}{h^2}\right) \tag{16a}$$

$$\sigma_{yz} = \frac{3}{2}\frac{S_y}{h}\left(1 - \frac{4z^2}{h^2}\right) \tag{16b}$$

As the off-diagonal terms corresponding to these stresses in the elasticity matrix [Eq. (14)] are zero, the transverse shear strains will have a distribution given by:

$$\epsilon_{xz} = r\bar{\theta}_x\left(1 - \frac{4z^2}{h^2}\right) \tag{17a}$$

$$\epsilon_{yz} = r\bar{\theta}_y\left(1 - \frac{4z^2}{h^2}\right) \tag{17b}$$

where $\bar{\theta}_x$ and $\bar{\theta}_y$ are the effective shear rotations and r is a constant. The constant r is evaluated by energy balancing as

$$\frac{1}{2}\int_{-h/2}^{h/2} \sigma_{xz}\epsilon_{xz} \cdot \mathrm{d}z = \frac{1}{2} S_x \bar{\theta}_x \tag{18}$$

By substituting Eqs. (16) and (17) in Eq. (18), one obtains

$$r = 5/4 \tag{19}$$

which is consistent with the shear coefficient, $\alpha = 6/5$, given by Reissner.[7] Equation (17), along with the value of r given by Eq. (19), is important as the incremental strains are obtained from incremental nodal displacements before proceeding with the plastic analysis.

Assuming the von Mises yield criterion to hold,

$$\phi(\{\sigma\}) = [\sigma_x^2 + \sigma_y^2 - \sigma_x\sigma_y + 3(\sigma_{xy}^2 + \sigma_{yz}^2 + \sigma_{zx}^2)]^{1/2} > \sigma_0 \tag{20}$$

where σ_0 is the yield stress in simple tension.

The gradient vector $\{\nabla\phi\}$ is given by:

$$\{\nabla\phi\} = \frac{1}{2\phi}\lfloor (2\sigma_x - \sigma_y)\ (2\sigma_y - \sigma_x)\ 6\sigma_{xy}\ 6\sigma_{yz}\ 6\sigma_{zx}\rfloor^T \tag{21}$$

The plastic analysis or the computation of plastic components of strain increments is carried out by applying the explicit elastoplastic strain matrix presented in Refs. 15 and 16. This matrix $[D_{ep}]$ gives the stress increments in terms of the imposed strain changes in the inelastic region as:

$$\{\Delta\sigma\} = [D_{ep}]\{\Delta\epsilon\} \tag{22}$$

and has the general form given by:

$$[D_{ep}] = [D] - \frac{1}{P}[D]\{\nabla\phi\}\{\nabla\phi\}^T[D] \tag{23}$$

where

$$P = A + \{\nabla\phi\}^T[D]\{\nabla\phi\} \tag{24}$$

and A is a function of the strain-hardening parameter and is equal to the slope of the universal stress-strain curve. The matrix $[D_{ep}]$ is a function of the stress state and Eq. (22) satisfies linearity in addition to normality and hardening law.

Numerical studies indicate that it is sufficiently accurate to evaluate $[D_{ep}]$ at stress values $\{\sigma\}_e$ given by the total strain increments

$$\{\sigma\}_e = \{\sigma\} + \{\Delta\sigma\}_e = \{\sigma\} + [D]\{\Delta\epsilon\} \tag{25}$$

where $\{\sigma\}$ is the initial stress state. It is also sufficient to evaluate just the actual stress increments given by Eqs. (22) and (23). That is, the plastic components of strain need not be calculated since Eq. (13) can be rewritten as:

$$\{\Delta F_p\}_j = \int_{V_j} [B]_j^T (\{\Delta\sigma\}_e - \{\Delta\sigma\}) \cdot \mathrm{d\ vol} \tag{26}$$

where the substitution

$$[D]\{\Delta\epsilon_p\} = \{\Delta\sigma\}_e - \{\Delta\sigma\} \tag{27}$$

is introduced.

Numerical Aspects

The inelastic response is found by numerically integrating Eq. (11) and by modifying the last term on the right-hand side of Eq. (11) at every step. For this purpose, a fourth-order Runge-Kutta procedure due to Gill[17] is made use of in the present work. At every time-step, the incremental nodal displacements are obtained and from these the strain increments in each element can be evaluated. Assuming the strain changes to be purely elastic, trial stress increments are computed and the resulting stress state is checked for yielding. For the points that have yielded, the stress increments are modified using elastoplastic relations. The process is repeated for all the analysis points in all the elements and, simultaneously, the equivalent incremental nodal forces are computed. Once the right-hand side of Eq. (11) is updated, accelerations at the end of the current time-step can be obtained using the equations of motion. Thus, we will have the necessary parameters to proceed to the next time step. A more complete description of the numerical procedure is given in Ref. 12. The volume integral of Eq. (26) is evaluated by numerical quadrature. Thus Eq. (26) is rewritten, for computational purposes, as

$$\{\Delta F_p\}_j = \sum_{k=1}^{n} [B]_{jk}^T (\{\Delta\sigma\}_e - \{\Delta\sigma\}) \cdot w_k \tag{28}$$

where n is the number of integration points and w_k is the weight associated with the kth integration point.

The convergence characteristics of the plate problem are studied with respect to the mesh size (number of elements) and the number of integration points. For studying the effect of mesh size, one-quarter of a plate has been idealized with 1×1, 2×2, 3×3, and 4×4 meshes and responses of a clamped plate were found under impulsive and step-load conditions. In both cases, the 3×3 mesh has been found to predict the peak displacement within about 5% of the converged value (Fig. 1a). The dependence of the response on the number of depthwise integration points (N_z) is shown in Fig. 1b. It is seen that the peak displacement is almost insensitive to N_z and $N_z = 3$ appears to yield satisfactory results throughout the range. As such, $2\times2\times3$ (length × breath × depth) integration points are used for each element in the subsequent problems. Inelastic responses of simply supported and clamped plates subject to uniform pressure load and uniform impulse were obtained. To estimate the contribution of transverse shear effects, responses were also computed by using a thin plate element presented by Bogner et al.[10] The numerical procedure remains the same except that the yield criterion for thin plates is:

$$\phi(\{\sigma\}) = (\sigma_x^2 + \sigma_y^2 - \sigma_x\sigma_y + 3\sigma_{xy}^2)^{1/2} > \sigma_0 \tag{29}$$

and the elastoplastic matrix $[D_{ep}]$ is altered correspondingly.

As the check on the procedure, the response of clamped rectangular plates to uniform impulse were computed and

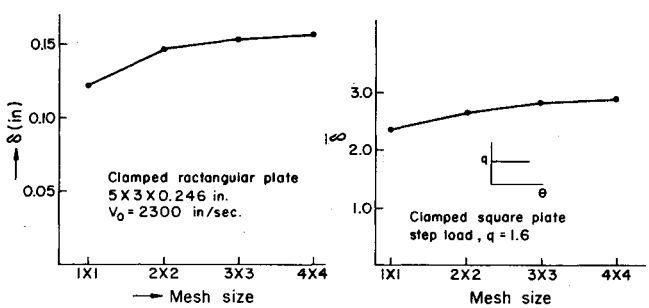

a) Peak displacemet with mesh size

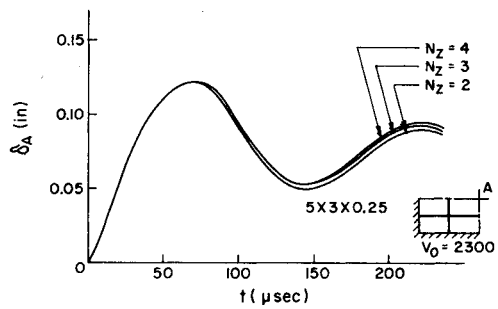

b) Peak displacement with number of integration points

Fig. 1 Convergence characteristics of plates.

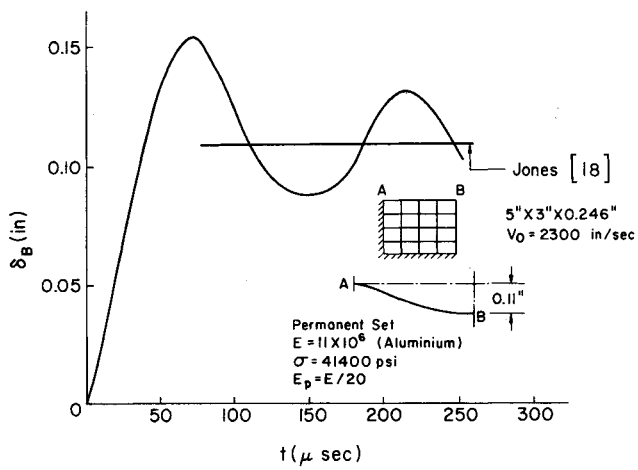

Fig. 2 Response of a clamped rectangular plate to an impulse.

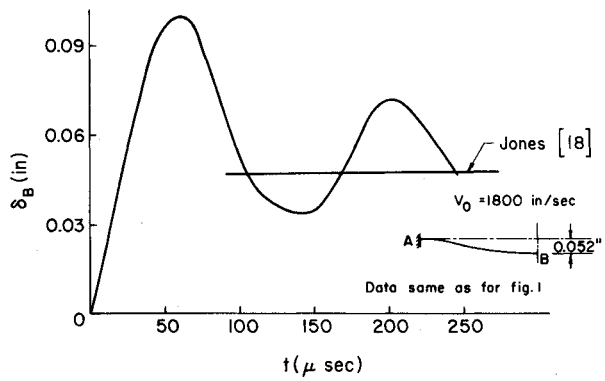

Fig. 3 Response of a clamped rectangular plate.

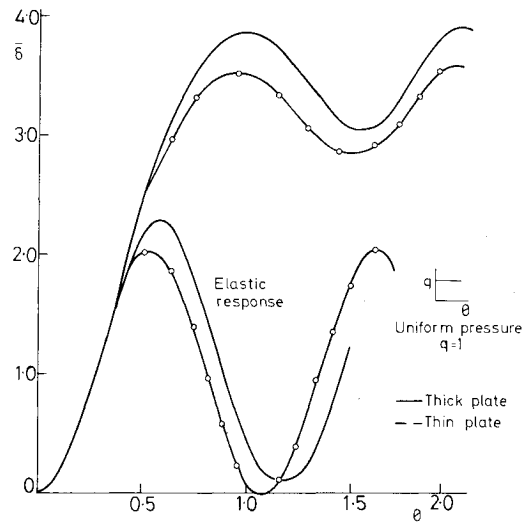

Fig. 4 Response of a simply supported thick plate, $a/h = 10$.

compared with the experimental value of permanent deformation reported by Jones.[18] These are presented in Figs. 2 and 3. In these problems, 16 elements (with 40 degrees of freedom) were used in one-quarter of a plate and the time-step size used was one-hundredth of the fundamental period. It can be seen that the equilibrium positions predicted by the present procedure agree well with the reported values.

Results

The response behavior of thick plates is presented in Figs. 4-8 in terms of the nondimensional parameters q (applied pressure), $\bar{\delta}$ (central displacement), θ (time), and λ (impulse) defined as:

$$q=\frac{p}{p_y},\quad \bar{\delta}=\frac{\delta}{q\cdot\delta_y},\quad \theta=\frac{t}{T_1},\quad \lambda=\frac{V_0}{V_r},\quad V_r=\frac{p_y T_1}{10m}$$

Here p,δ,t, and V_0 are, respectively, the applied pressure, actual response, time, and initial velocity; p_y is the static yield load, that is, the minimum load at which the maximum value of the moment reaches the fully plastic value, $M_0=\sigma_0 h^2/4$; δ_y is the static deflection corresponding to p_y; T_1 is the fundamental period; and m is the mass per unit area of the plate. The reference velocity V_r is equivalent to the load p_y acting on the plate over a duration ($T_1/10$), and is given by:

$$V_r=k\sigma_0\Big/\sqrt{\frac{\rho E}{(1-\nu^2)}}$$

where k is a constant depending on the boundary conditions and the aspect ratio of the plate. In the case of impulsive loading, the nondimensional response is defined as:

$$\bar{\delta}=\delta/(\lambda\delta_y)$$

Table 2 Reference input and response parameters

Serial no.	Description	p_y	δ_y	T_1	k
1	Simply supported square plate of side a	$\dfrac{M_0}{0.048a^2}$	$0.00406c_1$	$\dfrac{c_2}{18.73}$	0.576
2	Clamped square plate of side a	$\dfrac{M_0}{0.053a^2}$	$0.00126c_1$	$\dfrac{c_2}{36}$	0.294

$$c_1=\frac{p_y a^4}{D}\qquad c_2=2\pi a^2\sqrt{m/D}\qquad D=\frac{Eh^3}{12(1-\nu^2)}$$

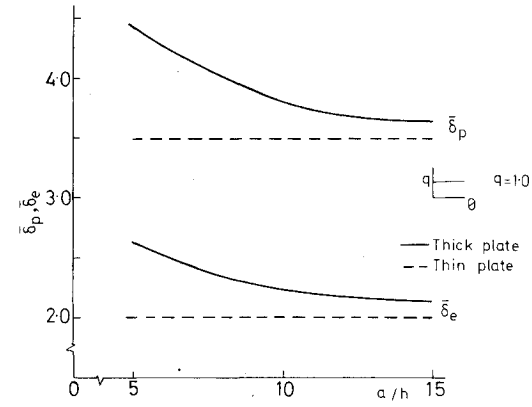

Fig. 5 Effect of (a/h) on the response of simply supported square plates.

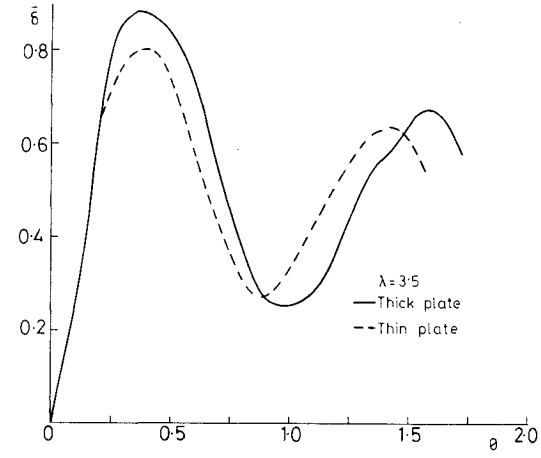

Fig. 6 Response of simply supported thick plate to impulse, $a/h = 5$.

Table 2 contains the values of p_y, δ_y, T_1, and k for simply supported and clamped square plates. The time step-size used in all the problems is $T_1/100$. These values are based on thin plate theory.

The response behavior of simply supported thick square plates is presented in Figs. 4-6 and the results are compared with those obtained from thin plate theory. In these cases, 88 degrees of freedom (9 elements) were used. For a thickness ratio (h/a) of 0.1, the effect of transverse shear is seen to correspond to an increase about 8% in the peak elastoplastic displacement. The influence of transverse shear on peak elastic response is also of the same order. This observation is seen to hold for other thickness ratios (Fig. 5).

It is seen from Fig. 6 that the influence of transverse shear is significantly less when the loading is impulsive. For a thickness ratio of 0.2 ($a/h=5$), the peak elastoplastic displacement is higher by about 10% and 25%, respectively, for impulsive and uniform step loading. The difference, which is quite significant, is possibly due to the dependence of response on the natural frequency. Inasmuch as the thick plate has a larger fundamental period, the reference initial velocity V_r is higher when transverse shear effects are included. Thus, for a given initial velocity V_0, the nondimensional value will be smaller.

For clamped plates, the influence of transverse shear is seen to be significantly higher (Fig. 7). For a thickness ratio of 0.1, the effect of transverse shear is seen to increase the peak displacement by over 30%. The static deflection computed for the same plate with the present finite element showed an increase of about 22% over that of a thin plate. As no results are available concerning clamped thick plates, even for static deflections, the present results could not be compared.

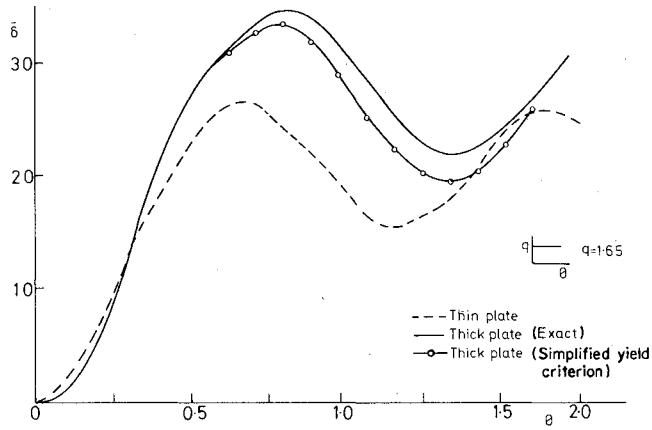

Fig. 7 Response of a clamped thick plate to uniform load, $a/h = 10$.

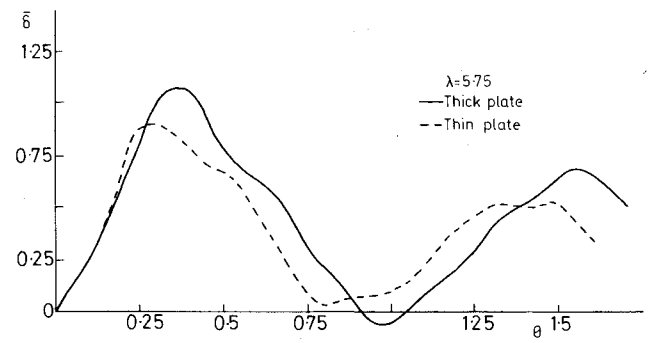

Fig. 8 Response of a clamped thick plate to an impulse, $a/h = 10$.

Figure 7 also contains the response of the thick plate computed by using a simplified yield criterion which does not contain transverse stresses. It is seen that the contribution of shear stresses is relatively less. This is predictable, since the transverse shear stresses, due to parabolic distribution, will have maximum values at the midddle plane where the in-plane stresses are zero. The response behavior of an impulsively loaded clamped plate (Fig. 8) is qualitatively in conformance with the result discussed for a simply supported plate. In the case of Figs. 7 and 8, the number of degrees of freedom used was 80 (9 elements).

The results just presented are for a uniform pressure of about $(\sigma_y/0.2)\,(h/a)^2$. This corresponds to a pressure of the order of 1800 psi for $a/h = 10$ and 7200 psi for $a/h = 5$ for mild steel with $\sigma_y = 36{,}000$ psi. These values represent, approximately, the pressures necessary for the structure to yield. In terms of displacements, the range of applicability of the present analysis is quite high. For $a/h = 10$, $\delta_y = 0.03\ h$ for a simply supported plate and still less for a clamped plate (for mild steel with $\sigma_y = 36{,}000$ psi and $E = 30 \times 10^6$ psi). For $a/h = 5$, $\delta_y = 0.0075\ h$. The dimensionless peak elastoplastic response is 4.0 for a simply supported plate, that is, $0.12\ h$, which is low enough not to introduce geometric nonlinearity. If the applied pressure is about four times p_y, the consideration of geometric nonlinearity may become important; but this pressure would be too high to be of any practical significance.

Conclusions

1) For a given thickness ratio, the influence of transverse shear on the peak elastoplastic displacement is maximized if the applied load is a uniform step-function of time. For such cases, the effect of transverse shear, in terms of percentage increase over that for thin plate, is of the same magnitude for peak elastic response also. In other words, the ratio of peak elastoplastic response to peak elastic response is independent of the thickness ratio and is equal to that of a thin plate.

2) The contribution of transverse shear stresses on yielding is relatively small.

3) From a practical viewpoint, the influence of transverse shear is too significant to be disregarded in the case of clamped plates.

Possible extensions of the present study include investigation of effects of stress concentration around holes of the same order of the thicknesses. Also, response of plates under asymmetric loading, where higher modes dominate, can be analyzed.

References

[1] Mindlin, R. D., "Influence of Rotary Inertia and Shear on Flexural Motions of Isotropic Rectangular Plates," *Journal of Applied Mechanics*, Vol. 18, March 1951, pp. 31-38.

[2] Mindlin, R. D., Schacknow, A., and Deresiewicz, H., "Flexural Vibrations of Rectangular Plates," *Journal of Applied Mechanics*, Vol. 23, Sept. 1956, pp. 431-436.

[3] Pryor, C. W. and Barker, R. M., "A Finite Element Analysis Including Transverse Shear Effects to Laminated Plates," *AIAA Journal*, Vol. 9, May 1971, pp. 912-917.

[4] Srinivas, S., Joga Rao, C. V., and Rao, A. K., "An Exact Analysis for Vibration of Simply Supported Homogeneous and Laminated Thick Rectangular Plates," *Journal of Sound and Vibration*, Vol. 12(2), June 1970, pp. 187-199.

[5] Rock, T. and Hinton, E., "Free Vibration and Transient Response of Thick and Thin Plates Using Finite Element Methods," *International Journal of Earthquake Engineering and Structural Dynamics*, Vol. 3, 1974, pp. 53-64.

[6] Felippa, C. A., "Refined Finite Element Analysis of Linear and Nonlinear Two Dimensional Structures," Ph.D. Dissertation, University of California, Berkeley, 1965.

[7] Reissner, E., "The Effect of Transverse Shear Deformation on the Bending of Elastic Plates," *Journal of Applied Mechanics*, Vol. 12, June 1945, pp. A69-A77.

[8] Zienkiewicz, O. C., *The Finite Element Method in Engineering Science*, McGraw Hill, London, 1971.

[9] Desai, C. S. and Abel, J. F., *Introduction to the Finite Element Method*, Van Nostrand Reinhold Co., New York, 1972.

[10] Bogner, F. K., Fox, R. L., and Schmidt Jr., L. A., "The Generation of Inter-Element Compatible Stiffness by the Use of Interpolation Formulas, Matrix Methods in Structural Analysis," AFFDL-TR-80, 1966, pp. 397-443.

[11] Salerno, U. L. and Goldberg, M. A., "Effect of Shear Deformation in the Bending of Rectangular Plates," *Journal of Applied Mechanics*, Vol. 27, March 1960, pp. 54-58.

[12] Raghavan, K. S., "Finite Element Studies on Inelastic Response of Beams and Plates," Ph.D. Thesis, Department of Mechanical Engineering, Indian Institute of Technology, Kanpur, India, Jan. 1977.

[13] Drucker, D. C., "Effect of Shear on Plastic Bending of Beams," *Journal of Applied Mechanics*, Vol. 23, Dec. 1956, pp. 515-521.

[14] Timoshenko, S. and Woinowsky-Kreiger, S., *Theory of Plates and Shells*, McGraw-Hill, New York, 1940.

[15] Yamada, Y., Yoshimura, N., and Sakurai, T., "Plastic Stress-Strain Matrix and its Application for the Solution of Elastic-Plastic Problems by the Finite Elements," *International Journal of Mechanical Science*, Vol. 10, May 1968, pp. 343-354.

[16] Zienkiewicz, O. C., Valliappan, S., and King, I. P., "Elasto-Plastic Solutions of Engineering Problems, Initial Stress, Finite Element Approach," *International Journal of Numerical Methods in Engineering*, Vol. 1, 1969, pp. 75-100.

[17] Gill, S., "A Process for Step-by-Step Integration of Differential Equations in an Automatic Digital Computing Machine," *Proceedings of Cambridge Philosophical Society*, Vol. 47, Jan. 1951, pp. 96-108.

[18] Jones, N., Uran, T. O., and Tekin, S. A., "Dynamic Plastic Behaviors of Fully Clamped Rectangular Plates," *International Journal of Solids and Structures*, Vol. 6, Dec. 1970, pp. 1499-1512.